J Solid State Electrochem (2001) 6: 8–15
DOI 10.1007/s100080000190

ORIGINAL PAPER

Xinming Qian · Ningyu Gu · Zhiliang Cheng
Xiurong Yang · Erkang Wang · Shaojun Dong

Methods to study the ionic conductivity of polymeric electrolytes using a.c. impedance spectroscopy

Received: 10 August 2000 / Accepted: 29 November 2000 / Published online: 15 August 2001

Abstract Composite polymeric electrolytes of PEO-$LiClO_4$-Al_2O_3 and PEO-$LiClO_4$-EC were prepared and the ionic conductivity by a.c. impedance was calculated using four different methods, and three kinds of representations of a.c. impedance spectra were adopted. The first is based on the Nyquist impedance plot of the imaginary part (Z'') versus the real part (Z') of the complex impedance. The second and the third correspond to the plots of imaginary impedance Z'' as a function of frequency (f), and the absolute value ($|Z|$) and phase angle (θ) as a function of f, respectively. It was found that the values of the ionic conductivity calculated using the three representations of a.c. impedance spectra are basically identical.

Keywords Ionic conductivity · Polymeric electrolyte · Impedance spectroscopy · Plasticizer

Introduction

Since the discovery of ionic conductivity in polymers containing inorganic salts, studies on solid polymeric electrolytes (SPEs) have been conducted all over the world because of the potential applications in batteries, electrochromic devices, sensors, and photoelectrochemical cells [1, 2, 3, 4]. These works are usually active in national projects such as USABC in the USA, NEDO in Japan, and JOULE in Europe [5]. Among these efforts of research and development, poly(ethylene oxide) (PEO) is commonly used as the polymer because of its chemical and electrochemical stability and the ability to dissolve high concentrations of salts to form a homogenous SPE [6]. The major drawback of PEO-based SPEs is that PEO shows a high tendency to crystallize or to form crystalline complexes and lower its ionic conductivity at room temperature. Various attempts have been made to improve the room temperature conductivity. One method of overcoming this problem is to use polymers in modified forms, such as polymer blends, copolymers, network polymers, and comb-like polymers [2, 7, 8]. Another method is to form composite SPEs by the addition of inorganic or organic additives [9, 10]. These methods may suppress the crystalline phase and the glass transition temperature (T_g) and enhance the amorphous phase, which will promote the ionic conductivity.

The investigation of the ionic conductivity of SPEs can be accomplished with the help of impedance spectroscopy. In fact, a.c. impedance spectroscopy has been a strategic analytical method employed in basic and applied electrochemistry as well as in the general field of materials science [11]. In the impedance measurements, a sinusoidal potential is applied and the impedance and the phase shift of the current are measured. The Nyquist impedance plot (Z'-Z'' plot) can be used to determine the appropriate equivalent circuit and to estimate the values of the circuit parameters which reflect the carrier transport properties and the reaction in the electrode interface [12]. Many authors have used the Nyquist impedance plot to elucidate the mechanisms of ionic processes taking place on the polymeric films and to obtain the bulk resistance of SPEs [13, 14, 15, 16, 17]. Besides the use of the equivalent circuit to estimate the bulk resistance of SPEs, there are several approaches to also determine the ionic conductivity of the SPEs, especially under situations when the impedance spectra become deformed.

In this paper, Al_2O_3 particles and ethylene carbonate (EC) were used as the additives to increase the room temperature ionic conductivity of PEO-based SPEs. With the changes of the additive concentration and the experiment temperature, the impedance spectra

X. Qian · N. Gu · Z. Cheng · X. Yang · E. Wang · S. Dong (✉)
Laboratory of Electroanalytical Chemistry,
Changchun Institute of Applied Chemistry,
Chinese Academy of Sciences, Jilin,
Changchun 130022, P.R. China
E-mail: dongsj@ns.ciac.jl.cn
Tel.: +86-431-5689711
Fax: +86-431-5689711

change to a shape different from an ideal one. To obtain the rational value of the ionic conductivity, different methods were used to estimate the bulk resistance. It is found that the values of the ionic conductivity calculated from different methods are identical.

Experimental

Preparation of $(PEO_1)_{10}LiClO_4$-Al_2O_3 and $(PEO_2)_{16}LiClO_4$-EC samples

PEO with different molecular weights [PEO_1 ($M_w = 10^4$) and PEO_2 ($M_w = 5\times10^5$)], Al_2O_3 ($d = 300$ nm), EC, and $LiClO_4$ were from Aldrich and were used as received. PEO and $LiClO_4$ were dried in a vacuum oven for 48 h at 50 °C and 72 h at 120 °C, respectively. Acetonitrile (Beijing Chemcal Plant) was dried by the addition of 4 Å molecular sieves before use and then was used to dissolve PEO. Pt and stainless steel (SS) were cut into specified plates that were used as collecting electrodes.

The SPE samples were prepared according to a procedure described elsewhere [10]. The additives Al_2O_3 and EC are the weight percent of $PEO_1 + LiClO_4$ and $PEO_2 + LiClO_4 + EC$, respectively. An appropriate amount of Al_2O_3 particles ($W = 25\%$) was firstly dispersed in acetonitrile solution in an ultrasonic cell for 20 min. For the preparation of $(PEO_1)_{10}LiClO_4$-Al_2O_3 (O:Li = 10:1) and $(PEO_2)_{16}LiClO_4$-EC (O:Li = 16:1) samples, stoichiometric amounts of $PEO_1 + LiClO_4 + Al_2O_3$ and $PEO_2 + LiClO_4 + EC$ were mixed in two small glass reactors, and then acetonitrile was added to form about 5 mass% suspensions. The mixtures were stirred magnetically for about 10 h until a homogenous suspension was obtained. For the SPE thin films, the suspension obtained was dropped into a home-built cell [18], and then the solvent was left to evaporate slowly at room temperature. The resultant films were then dried in a vacuum oven at 30 °C for 48 h. The dry films were cut to the required size as samples and then were sandwiched between Pt or SS blocking electrodes. All samples were evaporated under vacuum for 24 h prior to measurements.

A.c. impedance spectra measurements

The impedance measurements were carried out using a Solartron 1250 frequency analyzer coupled to a 1286 electrochemistry interface over the frequency range 0.1 Hz to 65,535 Hz. The impedance data were then transferred to the Z-polt/Z-view software package (Scribner Associates, Southern Pines, NC, USA). For $(PEO_2)_{16}LiClO_4$-EC samples the conductivity measurements were performed from room temperature to about 100 °C. The samples were kept in a temperature-controlled oven with a flow of dry N_2. Before each impedance measurement the cell was kept at the testing temperature for at least 30 min to allow thermal equilibration.

Results and discussion

The ionic conductivity of the SPE can be calculated by the following equation:

$$\delta = \frac{1}{R_b}\frac{d}{S} \tag{1}$$

where δ is the ionic conductivity, d is the thickness of the SPE thin film, S is the area of electrodes contacting with the SPE film, and R_b is the bulk resistance.

Ionic conductivity calculated from the equivalent circuit

In a Nyquist impedance plot, the real part of the impedance is plotted against the imaginary part for data collected at a series of frequencies. To analyze the characteristics of the Nyquist impedance plot, an equivalent circuit is often used because it is simple, fast, and can provide a complete picture of the system [19]. The bulk resistance of the SPE is one of the quantities that can be derived from the equivalent circuit.

Figure 1 shows the Nyquist impedance plots for the Pt/$(PEO_1)_{10}LiClO_4$/Pt and Pt/$(PEO_1)_{10}LiClO_4$-Al_2O_3/Pt structures. It is clearly seen that there is a compressed semicircle in the high-frequency range and an inclined straight line in the low-frequency range for each sample. These diagrams deviate from an ideal impedance spectrum that usually exhibits a standard semicircle at the high-frequency section and a vertical line at the lower-frequency section. The deformed semicircle and the inclined line for the polymeric film/electrode system may result from the irregular thickness and morphology of the polymeric film and the roughness of the electrode surface [20, 21]. To analyze the phenomenon a "constant phase element" (CPE) [22] was used in the equivalent circuit, which was designed as shown in Fig. 2. R_b and C_g denote the bulk resistance and the geometry capacity of the SPE, respectively, CPE_1 represents the characteristics of the double layer between the electrolyte/electrode interface, and CPE_2 represents the effects of dipolar relaxation. The high-frequency semicircle reflects the combination of R_b, C_g, and CPE_2, while the straight line after the semicircle can be explained with CPE_1 corresponding to the double layer capacity of an inhomogeneous electrode surface [20].

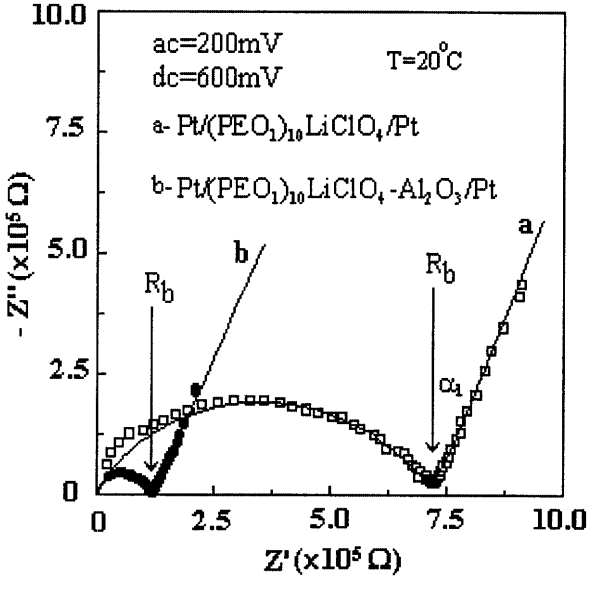

Fig. 1 Nyquist impedance plots for (*a*) Pt/$(PEO_1)_{10}LiClO_4$/Pt and (*b*) Pt/$(PEO_1)_{10}LiClO_4$-Al_2O_3/Pt structures at room temperature

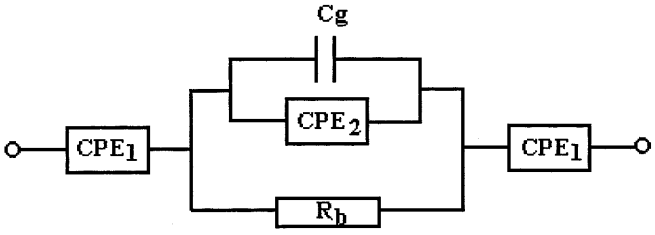

Fig. 2 An equivalent circuit to interpret the Nyquist impedance plots in Fig. 1

The impedance of the CPE is given by an empirical formula [23]:

$$Z_{\mathrm{CPE}} = A(j\omega)^{-n} \tag{2}$$

$$\alpha = (1-n)\frac{\pi}{2} \tag{3}$$

where A is the inverse of the capacitance only when $n=1$, and n is related to α (the deviation from the vertical line in Nyquist impedance plot); $n=1$ indicates a perfect capacitance, and a lower n value directly reflects the roughness of the electrode used [23, 24, 25]. In the software used in this paper the CPE is defined by two parameters, CPE-T and CPE-P. CPE-P is a parameter that equals n in Eqs. 2 and 3, while CPE-T indicates the value of the capacitance of the CPE element. If CPE-P equals 1, then Eq. 2 is identical to that of a capacitor. If CPE-P equals 0.5, a 45° line is produced on the Nyquist impedance plot. When a CPE is placed in parallel to a resistor, a depressed semicircle is produced.

Using the equivalent circuit shown in Fig. 2, the impedance data for $Pt/(PEO_1)_{10}LiClO_4/Pt$ and $Pt/(PEO_1)_{10}LiClO_4$-Al_2O_3/Pt were fitted as shown in Fig. 1 (solid line). As can be seen, the theoretical line calculated from the estimated values shows good correlation with the experimental data. The extracted parameters for the circuit elements are summarized in Table 1. Sample I is $(PEO_1)_{10}LiClO_4$ and sample II is $(PEO_1)_{10}LiClO_4$-Al_2O_3. CPE_1-T and CPE_2-T indicate the capacitance of CPE_1 and CPE_2, respectively. CPE_1-P and CPE_2-P are the parameters of CPE_1 and CPE_2, respectively; its value is equal to n shown in Eqs. 2 and 3. α_1 indicates the deviation of the lower-frequency inclined line from the vertical, and α_2 indicates the change of the phase angle of CPE_2, which shows the compressed high-frequency semicircle; ϵ is the standard deviation between the original data and the calculated spectrum. The bulk resistance of $Pt/(PEO_1)_{10}LiClO_4/Pt$ and $Pt/(PEO_1)_{10}LiClO_4$-Al_2O_3/Pt is 723,700 Ω and 120,960 Ω, respectively. The bulk resistance allows us to obtain the ionic conductivity using Eq. 1. It is clear that the ionic conductivity of the $(PEO_1)_{10}LiClO_4$ system is increased by the addition of Al_2O_3 particles.

Bulk resistance obtained from Nyquist impedance plot directly

In the Nyquist impedance plot, the low-frequency straight line and the high-frequency semicircle correspond to the electrolyte/electrode interface impedance and bulk electrochemistry impedance, respectively [26]. At higher frequencies, Bellucci et al. [21] considered that the total capacitance (C) becomes the total of C_g and the capacity fraction of CPE_2. The equivalent circuit of Fig. 2 is symbolized by the parallel combination of R_b and C, and the impedance corresponding to the bulk electrolyte is expressed as Eq. 4:

$$Z = \frac{R_b}{1 + i\omega R_b C} \tag{4}$$

The locus of Eq. 4 is a semicircle centered at $R_b/2$ on the real axis with a radius of $R_b/2$. At low frequencies, C_g and CPE_2 are considered to be open. The equivalent circuit of Fig. 2 can be reduced by R_b in series with CPE_1. The impedance (Z) of the reduced equivalent circuit can be written as Eq. 5:

$$Z = R_b + Z_{\mathrm{CPE_1}} \tag{5}$$

Many authors have obtained the bulk resistance R_b in the Nyquist impedance plot directly [27, 28, 29]. The low-frequency end of the semicircle and the high-frequency end of the straight line coincide with R_b. From Fig. 1, R_b values for $(PEO_1)_{10}LiClO_4$ and $(PEO_1)_{10}LiClO_4$-Al_2O_3 are 721,960 Ω and 120,009 Ω, respectively. Using Eq. 1, the ionic conductivities for $Pt/(PEO_1)_{10}LiClO_4/Pt$ and $Pt/(PEO_1)_{10}LiClO_4$-Al_2O_3/Pt are $9.065\times10^{-7}\ \Omega^{-1}\,cm^{-1}$ and $4.804\times10^{-6}\ \Omega^{-1}\,cm^{-1}$, respectively, which is almost the same as the values obtained above.

Table 1 Parameters for the circuit elements evaluated by fitting the impedance data of Fig. 1 to the equivalent circuit show in Fig. 2

Sample[a]	Fitted parameters									Calculated conductivity	
	CPE_1-T (10^{-5} F)	CPE_1-P (n_1)	α_1 (°)	CPE_2-T (10^{-8} F)	CPE_2-P (n_2)	α_2 (°)	C_g (10^{-10} F)	R_b (10^5 Ω)	ϵ (10^{-3})	d/S (cm^{-1})	δ ($10^{-6}\ \Omega^{-1}\,cm^{-1}$)
I	7.258	0.75	0.125π	4.5	0.625	0.187π	3.5	7.237	4.88	0.6545	0.904
II	7.1	0.73	0.135π	2.2	0.825	0.0875π	5.0	1.2096	3.74	0.5769	4.77

[a]Sample I is $(PEO_1)_{10}LiClO_4$ and sample II is $(PEO_1)_{10}LiClO_4$-Al_2O_3

Bulk resistance obtained
from the imaginary impedance

From Eq. 4, the imaginary impedance is given by Eq. 6:

$$Z'' = \frac{\omega C R_b^2}{1 + \omega^2 C^2 R_b^2} \tag{6}$$

Figure 3 shows the Z''-f plots for the Pt/$(PEO_1)_{10}LiClO_4$/Pt and Pt/$(PEO_1)_{10}LiClO_4$-Al_2O_3/Pt structures. Taking a derivation of Z'' with respect to angular frequency, we obtain [30, 31, 32]:

$$\frac{dZ''}{d\omega} = \frac{CR_b^2(1 - \omega^2 R_b^2 C^2)}{(1 + \omega^2 R_b^2 C^2)} \tag{7}$$

Equation 7 is equal to zero when the following is met:

$$\omega = \frac{1}{R_b C} \tag{8}$$

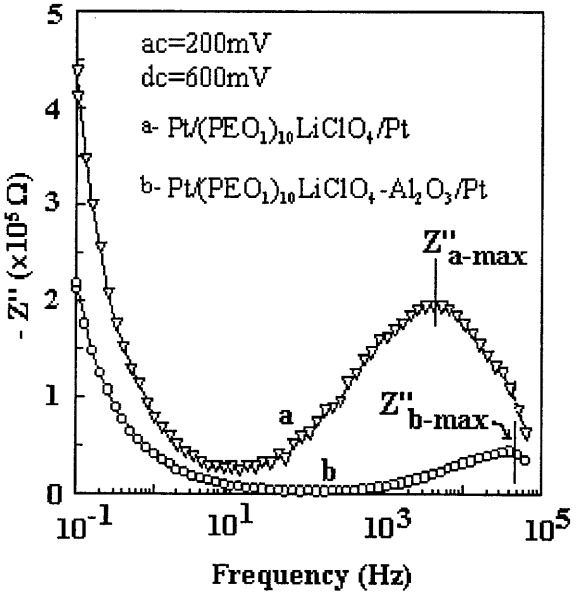

Fig. 3 Imaginary impedance as a function of frequency for (*a*) $(PEO_1)_{10}LiClO_4$ and (*b*) $(PEO_1)_{10}LiClO_4$-Al_2O_3 SPE at room temperature

By combining Eqs. 7 and 8, we obtain:

$$Z''_{max} = \frac{R_b}{2} \tag{9}$$

and thus the unknown resistance R_b is obtained directly from Z''_{max}. However, the measured centers of the high-frequency semicircle lie apparently below the Z' axis in the present study, as shown in Fig. 1. In order to analyze this compressed semicircle, Watanabe [26] introduced a phase angle β into Eq. 9:

$$Z'' = \frac{1}{2} R_b \frac{\sin(\beta\pi/2)}{\cosh(\beta \ln \omega R_b C_g) + \cos(\beta\pi/2)} \tag{10}$$

Equation 10 seems difficult to be understood. In fact the compressed semicircle can be looked upon as a part

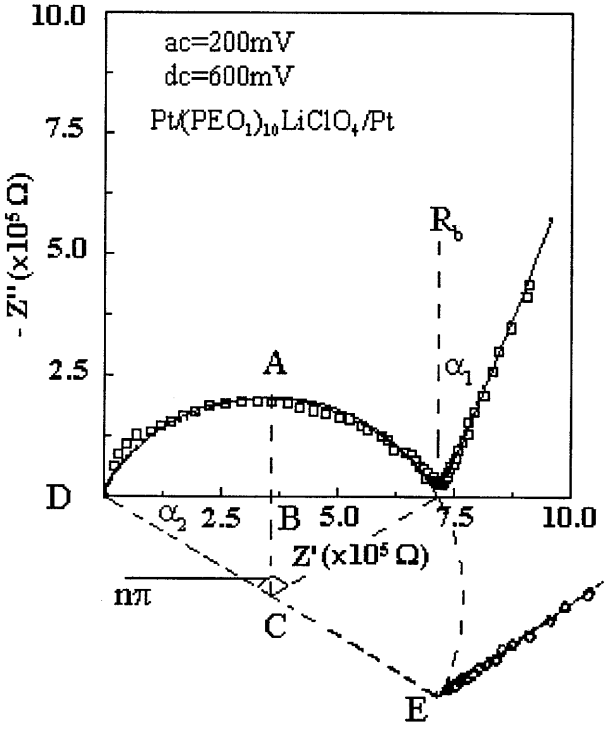

Fig. 4 A schematic diagram of the rotated impedance spectrum for the $(PEO_1)_{10}LiClO_4$ sample

Table 2 Conductivity values calculated by different methods for $(PEO_1)_{10}LiClO_4$ and $(PEO_1)_{10}LiClO_4$-Al_2O_3 polymeric electrolytes

Method[a]	Sample[b]	Z''_{max}			R_b (10^5 Ω)	d/S (cm^{-1})	δ (10^{-6} Ω^{-1} cm^{-1})
		Z''_{max} (10^5 Ω)	n(CPE_2-P)	α_2			
Method 1	A	–	–	–	7.237	0.6545	0.904
	B	–	–	–	1.2096	0.5769	4.77
Method 2	A	–	–	–	7.2196	0.6545	0.9065
	B	–	–	–	1.20009	0.5769	4.804
Method 3	A	1.9509	0.626	0.187π	7.29487	0.6545	0.897
	B	0.44585	0.825	0.0875π	1.177	0.5769	4.901

[a]Method 1: bulk resistance calculated from the equivalent circuit. Method 2: bulk resistance obtained from Nyquist impedance plots directly. Method 3: bulk resistance obtained from the imaginary impedance

[b]A represents $(PEO_1)_{10}LiClO_4$, and B represents $(PEO_1)_{10}LiClO_4$-Al_2O_3

of an ideal semicircle which has rotated a certain angle clockwise, as shown in Fig. 4. In this figure, n has the same meaning as β in Eq. 10, which is equal to the fitting data of CPE_2-P; α can be calculated using Eq. 3. The length of A to B (shown in Fig. 4) denotes the value of Z''_{max} shown in Fig. 3. It is clear that Z''_{max} can be expressed as Eq. 11 based on the analysis of Fig. 4:

$$Z''_{max} = \frac{R_b}{2}\frac{1-\sin\alpha}{\cos\alpha} \tag{11}$$

Then the calculation of R_b is straightforward since the experimentally determined value of Z''_{max} is always characterized by a distinct peak in the frequency range [33, 34, 35]. From Fig. 3, the maximum of $Z''_{a\text{-}max}$ is $1.9509\times10^5\,\Omega$ and $Z''_{b\text{-}max}$ is $4.4585\times10^4\,\Omega$, which indicates that R_b for $(PEO_1)_{10}LiClO_4$ and $(PEO_1)_{10}LiClO_4$-Al_2O_3 are 729,487 Ω and 117,700 Ω, corresponding to the ionic conductivities of $8.97\times10^{-7}\,\Omega^{-1}\,cm^{-1}$ and $4.901\times10^{-6}\,\Omega^{-1}\,cm^{-1}$, respectively. The ionic conductivity is the same as that calculated from Eq. 10. Compared with the calculation using Eq. 10, the estimation of R_b using Eq. 9 inferred in this paper is simple and easy. The ionic conductivity values calculated from the above three different methods for $(PEO_1)_{10}LiClO_4$ and $(PEO_1)_{10}LiClO_4$-Al_2O_3 polymeric electrolytes are summarized in Table 2. It is clear that the value of the ionic conductivity obtained from the different methods coincide with each other. Although the methods for the estimation of R_b from the Nyquist plot and the imaginary impedance cannot determine the standard error of R_b, they are still extensively used in the investigation of polymeric electrolytes [21, 22, 26, 27, 28, 29, 30, 31, 32].

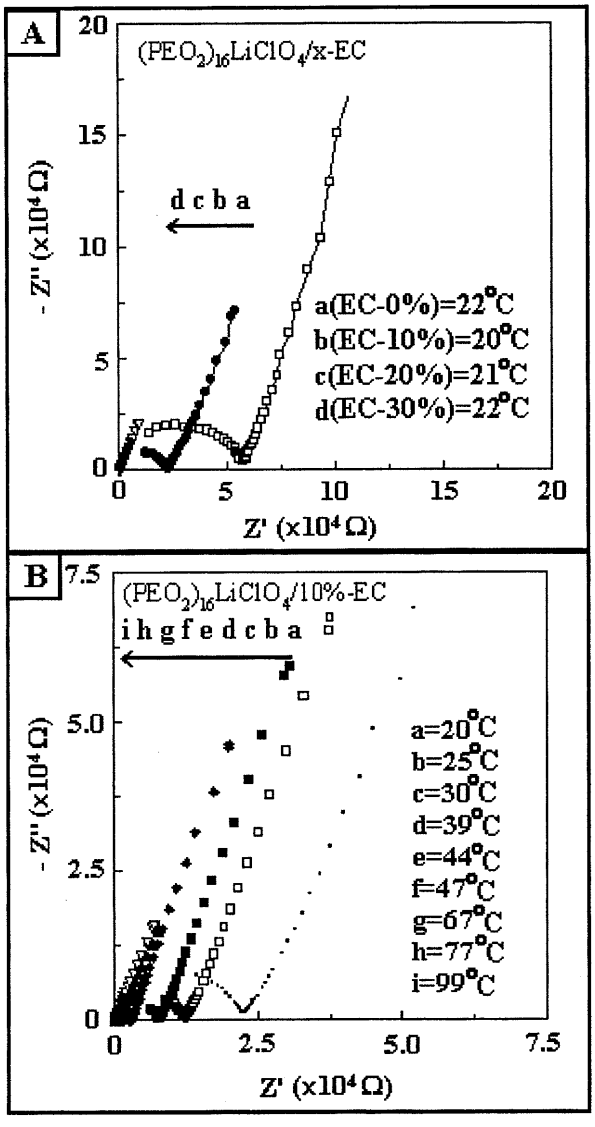

Fig. 5 Nyquist impedance plots for **A** $(PEO_2)_{16}LiClO_4$-EC with different EC concentrations at room temperature, and **B** $(PEO_2)_{16}LiClO_4$-EC(10%) at different temperatures

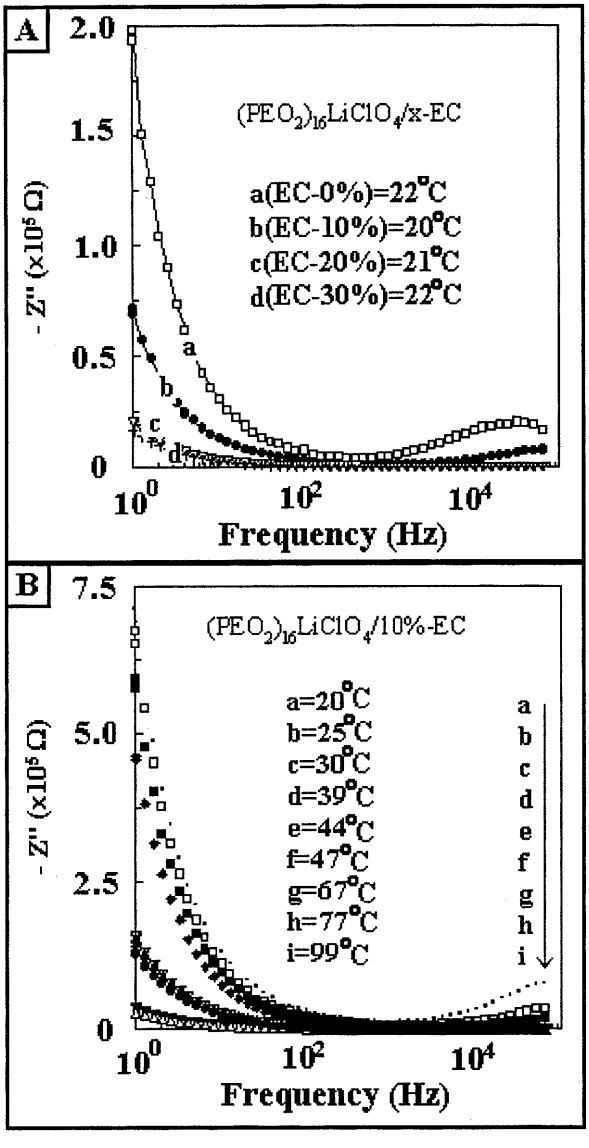

Fig. 6 Imaginary impedance as a function of frequency for **A** $(PEO_2)_{16}LiClO_4$-EC with different EC concentrations at room temperature, and **B** $(PEO_2)_{16}LiClO_4$-EC(10%) at different temperatures

Ionic conductivity calculated from $|Z|$ versus frequency and phase angle versus frequency plots

Figure 5 shows the Nyquist impedance plots for $(PEO_2)_{16}LiClO_4$-EC plasticized polymeric electrolytes using SS blocking electrodes. It is found that the high-frequency semicircles disappear gradually with increasing EC concentration and increasing temperatures. The decreased bulk resistance indicates that the ionic conductivity increases with the increasing EC concentration and the experimental temperature. This change in the Nyquist impedance plot makes it difficult to obtain the bulk resistance value directly from the plots of the serial samples.

Figure 6 shows the Z-f plots for the same samples as in Fig. 5. It is clearly seen that the maximum of Z'' in the plot becomes indistinguishable with the increase of EC concentration and the experimental temperature. This plot, as well as Fig. 5, cannot give the exact bulk resistance of these samples directly. As reported in the literature [29], the appearance of the high-frequency semicircle and the imaginary maximum peak of these samples with high plasticizer concentration or high experimental temperature should be higher than 100 kHz. However, this frequency limitation is beyond the instrument used in the present study. In such a case, an alternative method should be introduced to obtain the bulk resistance.

The plots of $|Z|$ versus f and θ versus f are the other representations of the complex impedance. These plots for $(PEO_2)_{16}LiClO_4$-EC samples with different EC concentrations and for $(PEO_2)_{16}LiClO_4$-EC(10%) at different temperatures are shown in Fig. 7 and Fig. 8, respectively. In Fig. 7 and Fig. 8A there is a plateau for each sample in the $|Z|$-f plot. With increasing the EC concentration and the experimental temperature, the value of the plateau intersect with the $|Z|$-axis decreases. On the other hand, for the θ-f plot, there is a minimum for each sample, which is shifted to higher frequency with the further addition of EC plasticizer and the increasing experimental temperature. The bulk resistance can be calculated using the absolute impedance and the phase angle as follows:

$$R_b = |Z| \cos\theta \tag{12}$$

$|Z|$ is obtained from the intersection of the extrapolated frequency-independent horizontal line and the $|Z|$ axis from Fig. 7 and Fig. 8A together with the phase angle (θ) corresponding to the minimum. The R_b values of each sample in Fig. 7 and Fig. 8 are shown in Table 3.

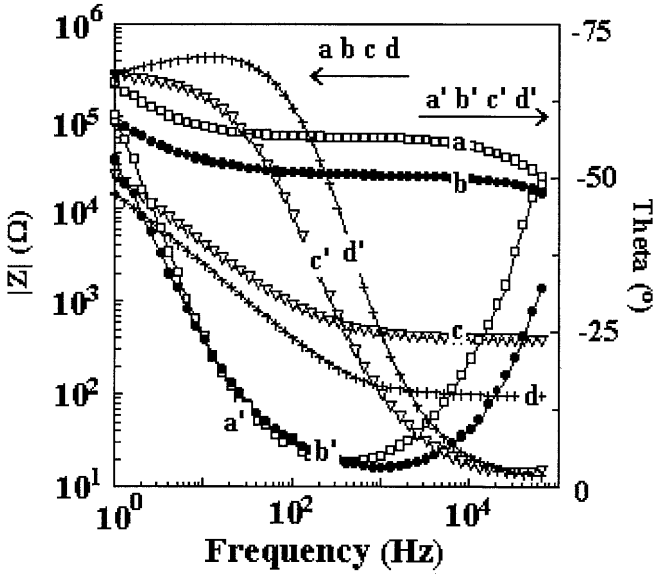

Fig. 7 Plots of absolute impedance and phase angle as a function of frequency for $(PEO_2)_{16}LiClO_4$-EC with different EC concentrations: (*a*) 0%, (*b*) 10%, (*c*) 20%, (*d*) 30%

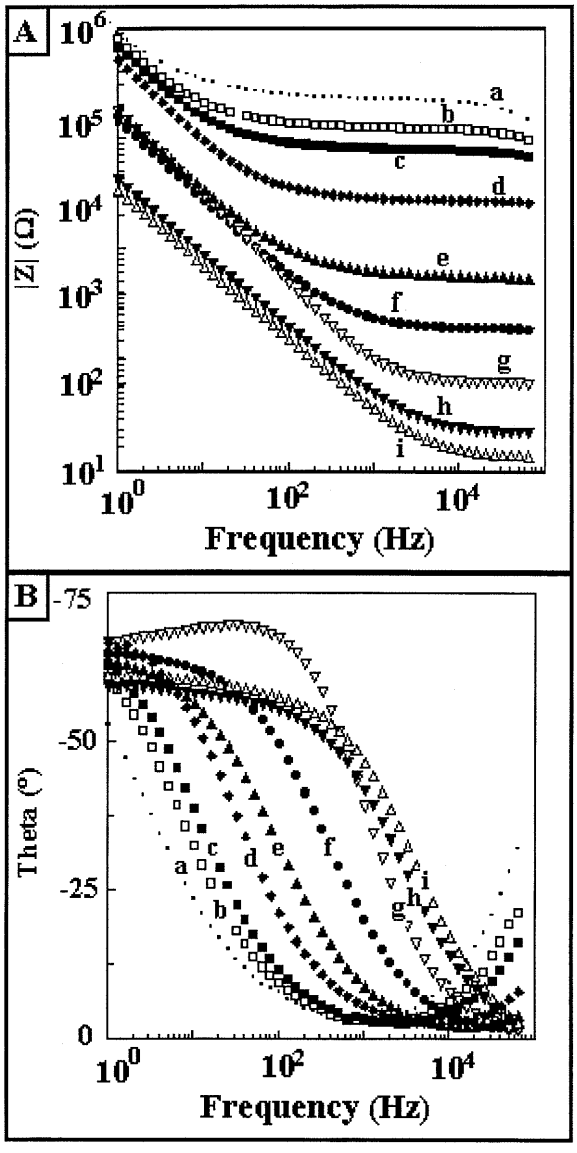

Fig. 8 **A** Plots of absolute impedance and **B** phase angle as a function of frequency for $(PEO_2)_{16}LiClO_4$-EC(10%) at different temperatures: (*a*) 20 °C, (*b*) 25 °C, (*c*) 30 °C, (*d*) 39 °C, (*e*) 44 °C, (*f*) 47 °C, (*g*) 67 °C, (*h*) 77 °C, (*i*) 99 °C

Table 3 Conductivity values calculated from different methods for $(PEO_2)_{16}LiClO_4$ and $(PEO_2)_{16}LiClO_4$-EC polymeric electrolytes

Sample	T (°C)	d/S (cm^{-1})	From [arrowvertex]Z[arrowvertex] vs. f and θ vs. f plots				From equivalent circuit	
			[arrowvertex]Z [arrowvertex] (Ω)	$-\theta$ (°)	R_b (Ω)	δ ($10^{-6}\ \Omega^{-1}\ cm^{-1}$)	R_b (Ω)	δ ($10^{-6}\ \Omega^{-1}\ cm^{-1}$)
EC 0%	22	0.0075	57569	4.0402	57425	0.13	57474	0.13
EC 20%	21	0.012	389.49	2.9294	388.98	30.8	414.1	29
EC 30%	20	0.01	143.23	2.2732	143.117	69.87	143.23	69.8
EC 10%	20	0.02	72499	3.3432	22460.7	0.8904	22382	0.894
EC 10%	25	0.02	12282	3.0185	12265	1.63	12173	1.64
EC 10%	30	0.02	7914.3	3.2813	7901	2.53	7872	2.54
EC 10%	39	0.02	2731	2.7128	2728	7.33	2740	7.3
EC 10%	44	0.02	558.87	2.2717	558.4	35.8	533.9	32.5
EC 10%	47	0.02	189.47	3.4068	189.1	105.8	184.86	108
EC 10%	67	0.02	61.422	2.3793	61.36	325.9	61.1	327
EC 10%	77	0.02	22.102	3.4876	22.06	907	22	909
EC 10%	99	0.02	13.831	4.0475	13.797	1449.5	13.78	1450

For comparison with the other methods, the results obtained from the equivalent circuit are also listed in Table 3. The results have three characteristics:

1. The ionic conductivity increases with the increasing EC concentration.
2. The ionic conductivity of $(PEO_2)_{16}LiClO_4$-EC(10%) increases with the experiment temperature.
3. The values of the ionic conductivity obtained using different methods are almost identical.

Comparing these four methods, the calculation of the ionic conductivity from the equivalent circuit is the most efficient way, but the other methods can also be used to estimate the bulk resistance of the polymeric electrolyte approximately.

Conclusion

Two kinds of composite polymeric electrolytes of PEO-$LiClO_4$-Al_2O_3 and PEO-$LiClO_4$-EC were prepared and their a.c. impedance spectra were measured using Pt or SS blocking electrodes. Four methods were introduced to calculate the ionic conductivity, based on the different representations of the a.c. impedance spectra. The equivalent circuit is an efficient tool to analyze the experiment data, and the bulk resistance in the circuit obtained from the fitting process can be used to calculate the ionic conductivity of SPEs.

Compared with the method of using the equivalent circuit, the bulk resistances obtained both from the Nyquist impedance plot and the Z'' versus f plot are convenient and straightforward. However, when the concentration of plasticizer and the experiment temperature are increased, the shape of the high-frequency semicircle changes gradually. In this case, the plot of $|Z|$ versus f can be used to obtain the value of the bulk resistance, and then the ionic conductivity can be calculated.

The results indicate that the ionic conductivity of the PEO-$LiClO_4$ system is increased by the addition of Al_2O_3 or EC additives and it is also increased on increasing the experimental temperature. The values of the ionic conductivity calculated from the different methods in the present study are almost identical.

Acknowledgements Financial support from the K.C. Wang Postdoctoral Research Award Fund of the Chinese Academy of Sciences and the China Postdoctoral Science Foundation are acknowledged. This work was supported by the National Natural Science Foundation of China (No. 29835120, 20075028).

References

1. MacGlashan GS, Andreev YG, Bruce PG (1999) Nature 398:792
2. Xu W, Siow KS, Gao ZQ, Lee SY (1998) Chem Mater 10:1951
3. Lightfoot P, Mehta MA, Bruce PG (1993) Science 262:883
4. Bach U, Lupo D, Comte P, Moser JE, Weissortel F, Salbeck J, Spreitzer H, Graetzel M (1998) Nature 395:583
5. Murata K, Izuchi S, Yoshihisa Y (2000) Electrochim Acta 45:1501
6. Whang WT, Bruce PG, Vincent CA (1993) J Chem Soc Faraday Trans 89:3187
7. Kim DW, Park JK, Gong MS (1995) J Polm Sci Part B Polym Phys 33:1323
8. Kata KI, Ito-Akita K, Ohno H (2000) J Solid State Electrochem 4:141
9. Wieczorek W, Raducha D, Zalewska A, Stevens JR (1998) J Phys Chem B 102:8725
10. Xu W, Deng ZH, Zhang XZ, Wan GX (1998) J Solid State Electrochem 2:257
11. Bandeira MCE, Franco CV, Martini E (1999) J Solid State Electrochem 3:210
12. Han DG, Choi GM (1999) Electrochim Acta 44:4155
13. Perez JH, Cardoso J, Manero O (1998) Polymer 39:6969
14. Ryoo HJ, Kim HT, Lee YG, Park JK, Moon SI (1998) J Solid State Electrochem 3:1
15. Choe HS, Carroll BG, Pasquariello DM, Abraham KM (1997) Chem Mater 9:369
16. Matanabe M, Itoh M, Sanui K, Ogata N (1987) Macromolecules 20:569
17. Albinsson I, Mellander BE, Stevens JR (1992) J Chem Phys 96:681
18. Qian XM, Du H, Lu HH, Bai YB, Li TJ, Tang XY (1999) Chin J Appl Chem 16(2):47
19. Han DG, Choi GM (1998) Solid State Ionics 106:71
20. Brug GJ, Van den Eeden ALG, Sluyters-Rehbach M, Sluyters JH, (1984) J Electroanal Chem 176:275

21. Bellucci F, Valentino M, Monetta T, Nicodemo L, Kenny J, Nicolais L, Mijovic J (1994) J Polym Sci Part B Polym Phys 32:2519
22. Dabrowska A, Wieczorek W (1994) Mater Sci Eng B 22:107
23. Zen JM, Ilangovan G, Jou JJ (1999) Anal Chem 71:2797
24. Ferloni P, Mastragostino M, Meneghello L (1996) Electrochim Acta 41:27
25. Sung HY, Wang YY, Wan CC (1998) J Electrochem Soc 145:1207
26. Watanabe M, Togo M, Sanui K, Ogata N, Kobayashi T, Ohtaki Z (1984) Macromolecules 17:2908
27. Watanabe M, Sanui K, Ogata N, Inoue F, Kobayashi T, Ohtaki Z (1985) Polym J 17:549
28. Vachon C, Labreche C, Vallee A, Besner S, Dumont M, Prud'homme J (1995) Macromolecules 28:5585
29. Munichandraiah N, Scanlon LG, Marsh RA, Kumar B, Sircar AK, (1995) J Appl Electrochem 25:857
30. Bellucci F, Valentino M, Monetta T, Nicodemo L, Kenny J, Nicolais L, Mijovic J (1995) J Polm Sci Part B Polym Phys 33:433
31. Mijovic J, Andjelic S, Fitz B, Zurawsky W, Mondragon I, Bellucci F, Nicolais L (1996) J Polm Sci Part B Polym Phys 34:379
32. Bellucci F, Maio V, Monetta T, Nicodemo L, Mijovic J (1996) J Polm Sci Part B Polym Phys 34:1277
33. Mijovic J, Yee CFW (1994) Macromolecules 27:7287
34. Mijovic J, Andjelic S, Yee CFW, Bellucci F, Nicolais L (1995) Macromolecules 28:2797
35. Mijovic J, Bellucci F, Nicodemo L (1995) J Electrochem Soc 142:1176